EVALUATION OF HOT ISOSTATIC PRESSING PARAMETERS ON THE OPTICAL AND BALLISTIC PROPERTIES OF SPINEL FOR TRANSPARENT ARMOR

Gary Gilde, Parimal Patel, James Sands and Philip Patterson
U.S. Army Research Laboratory, Attn. AMSRL-WM-MC
Aberdeen Proving Ground, MD 21005

David Blodgett, Donald Duncan, and Daniel Hahn
The Johns Hopkins University Applied Physics Laboratory
Laurel, MD 20723

ABSTRACT

The effect of different hot pressing and hot isostatic pressing temperatures and pressures on the optical properties of spinel was studied. Extinction coefficients of spinel samples were estimated by comparing the measured transmittance with the theoretical transmittance as calculated via a Sellmeier model. Results showed that the relative size of the scattering sites was large compared to the wavelengths of light (0.35 to 5.5 μm). Overall, increasing HIP temperature and pressure resulted in decreasing the optical extinction. The lower of two hot pressing temperatures (1620ºC versus 1650ºC) prior to HIPing resulted in lower scatter coefficients after HIPing; this effect was most significant in the infrared. The single shot and multi-shot ballistic properties of spinel based armor system have been evaluated. Compared to single crystal sapphire and polycrystalline ALON™, spinel has superior ballistic properties to that of sapphire and is comparable to ALON. Initial testing indicates that the multi-hit ballistic performance of sapphire is comparable to spinel.

I. INTRODUCTION

Transparent armor systems using spinel as the striking face have been known to be superior to glass based transparent armor systems since the early 1970's. It has not been available in sizes and shapes large enough to be fielded and has been too expensive to be used. The small sizes that could be made precluded multi-hit ballistic testing.

Beginning in 1996 the Army Research Laboratory (ARL) focused on making larger sized pieces of spinel available for testing and lowering the cost of manufacturing spinel. Technologies developed for manufacturing spinel were transferred to Technology Assessment and Transfer (Annapolis MD) under a CRDA. ARL and TA&T are continuing the development of spinel under a Cooperative Agreement. Figure 1. shows the recent history of the development of spinel by ARL. TA&T is now hot-pressing spinel plates in sizes up to 11" x 14" x 0.5". They have hot-pressed 9" x 14" curved plates.

With the larger spinel plates available ARL has been able to design transparent armor systems for multi-hit ballistic testing and validate these designs. Other materials such as ALON and sapphire have become available in sizes large enough to test in multi-hit configurations and comparisons can be made.

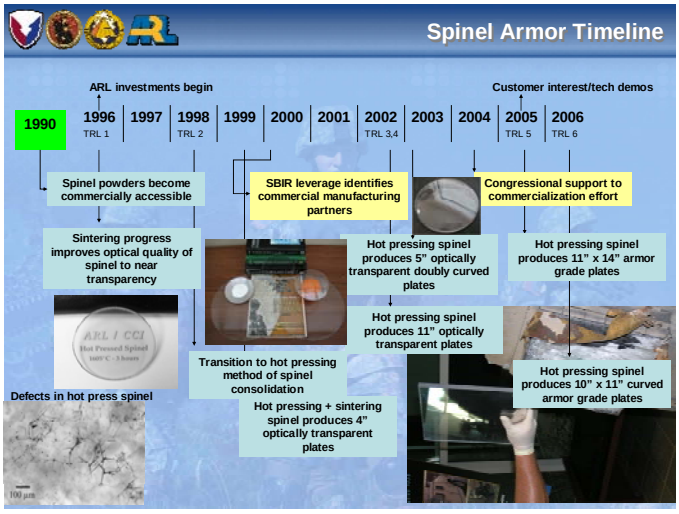

Figure 1. Time Line for the recent development of spinel armor by ARL.

Transparent magnesium aluminate spinel, $MgAl_2O_4$, has high strength, hardness, and the high temperature stability needed for applications such as advanced electromagnetic (EM) windows and transparent armor. The broad EM transmission window of spinel extends from almost 0.2 μm to 6 μm.[1] Despite many attempts to commercialize spinel, it is not available today as an optical material due to difficulties in consistently obtaining the desired transparency.

The spinel crystal structure is cubic and thus optically isotropic, allowing polycrystalline bodies to be fabricated without the severe scattering problems inherent in polycrystalline anisotropic materials. Spinel does not undergo any polymorphic transformations, so it is free of problems due to thermally induced phase changes. Extensive programs were carried out in the 1980's at the Johns Hopkins University Applied Physics Laboratory[2] and Honeywell Systems Research Center[3] to measure the properties of spinel, sapphire, AlON and yttria.

Results from the work by APL showed spinel has distinct optical property advantages over both sapphire and AlON. In contrast to cubic spinel, single crystal Al_2O_3 [sapphire] is anisotropic, and thus is birefringent, causing optical design problems for window applications. AlON has a shorter transmission cut-off in the 4.5 to 5.5 microns spectral region resulting in a significantly higher coefficient of absorption in that critical band. Based on these properties and the hope

Report Documentation Page

Form Approved
OMB No. 0704-0188

1. REPORT DATE	2. REPORT TYPE	3. DATES COVERED
01 NOV 2006	**N/A**	**-**

4. TITLE AND SUBTITLE	5a. CONTRACT NUMBER
Evaluation Of Hot Isostatic Pressing Parameters On The Optical And Ballistic Properties Of Spinel For Transparent Armor	5b. GRANT NUMBER
	5c. PROGRAM ELEMENT NUMBER
6. AUTHOR(S)	5d. PROJECT NUMBER
	5e. TASK NUMBER
	5f. WORK UNIT NUMBER
7. PERFORMING ORGANIZATION NAME(S) AND ADDRESS(ES) **U.S. Army Research Laboratory, Attn. AMSRL-WM-MC Aberdeen Proving Ground, MD 21005**	8. PERFORMING ORGANIZATION REPORT NUMBER
9. SPONSORING/MONITORING AGENCY NAME(S) AND ADDRESS(ES)	10. SPONSOR/MONITOR'S ACRONYM(S)
	11. SPONSOR/MONITOR'S REPORT NUMBER(S)

12. DISTRIBUTION/AVAILABILITY STATEMENT
Approved for public release, distribution unlimited

13. SUPPLEMENTARY NOTES
See also ADM002075., The original document contains color images.

14. ABSTRACT

15. SUBJECT TERMS

16. SECURITY CLASSIFICATION OF:			17. LIMITATION OF ABSTRACT	18. NUMBER OF PAGES	19a. NAME OF RESPONSIBLE PERSON
a. REPORT	b. ABSTRACT	c. THIS PAGE			
unclassified	**unclassified**	**unclassified**	**UU**	**8**	

that spinel can be fabricated at a considerably reduced cost over either AlON or sapphire, spinel is being developed for use in multimode windows and domes for a wide range of defense applications. It is also being investigated for optical lenses and transparent armor. For armor applications, it is the goal of being able to produce large panels, possibly up to 36″ in diameter through a low cost hot-pressing process that is driving the continued interest.

Previous work also has identified that hot-pressing followed by hot isostatic pressing (HIPing) is the most promising method for processing transparent spinel[4,5]. Previous work compared hot-pressing and sintering; the HIP conditions were not varied. Figure 2 shows a hot-pressed /HIPed spinel plate made using a typical HIP schedule. The current industry-accepted need for high HIP temperature and pressure limits the sizes of spinel that can be produced in commercially available HIPs. If the HIP temperature and pressure can be lowered to 1500ºC/ 100 MPa, HIPs with hot-zone diameters as large as 1.5 m are readily available. This is significantly larger than the 1 meter hot-presses that are commercially available. The goal of this program was to investigate the effect of HIP temperature and pressure on the optical properties of spinel and to thereby determine the feasibility of using low temperature, low pressure HIP cycles or eliminating the HIP cycle to produce spinel of the quality needed for transparent armor and electromagnetic window applications. In addition, two different hot-pressing temperatures (1620ºC and 1650ºC) are used to prepare the samples prior to HIPing so that the effects of different sample preparations on the final HIPed product may also be studied.

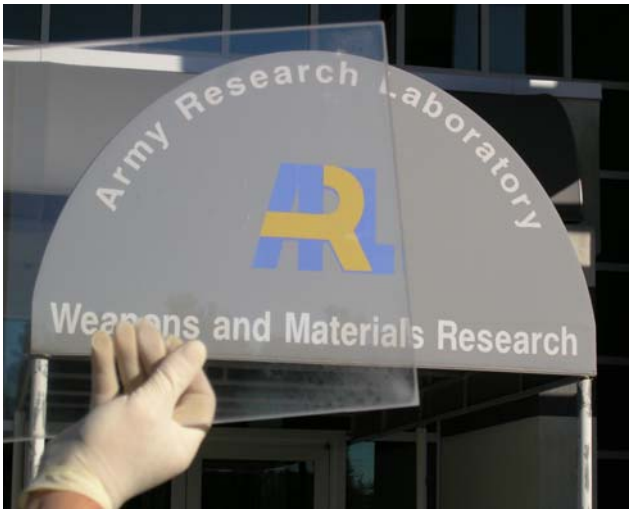

Figure 2. A hot-pressed spinel plate 11” x 14” made using a typical high temperature HIP cycle.

II. EXPERIMENTAL PROCEDURE

Hot-pressing was used to densify the spinel prior to HIPing. Spinel powder (Baikowsiki S30-CR, Charlotte NC) was mixed with 0.75 wt.% LiF (LITHCO, Bessemer, NC) by shaking with a TURBULA mixer (Glen Mills, Inc., Clifton, NJ) for 60 minutes in a high density polyethylene container. The powder was then sieved through a USA series 60 mesh polyester sieve. Three spinel circular billets 100 mm in diameter, 10 mm thick were hot-pressed using graphite dies and Grafoil liners. The hot-pressing pressure for all three billets was 20 MPa. The hot-pressing matrix used to prepare the samples for these experiments is shown in Table I. Sample C was hot-pressed using the same schedule as sample B except it was held at 1550ºC for 12 hours during the ramp down to room temperature. The three billets were polished to an optical finish by NU-TEX Precision Optical Corporation, Aberdeen, MD. From each billet, 6 pieces, each 25 mm diameter and 6 mm thick, were core drilled. These pieces were then HIPed for 6 hours at (1)1500ºC/100 MPa, (2)1500ºC/200 MPa, (3)1700ºC/100 MPa, (4)1700ºC/200 MPa, and (5)1900ºC/200 MPa (Table II). One piece (0) was kept in the as hot-pressed condition to be used as a control. The HIPed samples were then repolished by NU-TEX before any optical property measurements were made.

Table I. Hot-Pressing Matrix

Sample	Hot pressing pressure	Firing conditions
A	20 MPa	1620ºC, 3 hrs
B	20 MPa	1650ºC 3 hrs
C	20 MPa	1650ºC 3 hrs: 1550ºC 12hrs vacuum anneal

Table II. Hot Isostatic Pressing Matrix

HIP ID #	HIP Pressure	HIP Temperature
0 control	-	-
1	100 Mpa	1500ºC
2	200 Mpa	1500ºC
3	100 Mpa	1700ºC
4	200 Mpa	1700ºC
5	200 Mpa	1900ºC

Transmittance measurements were performed both with a conventional broadband spectrometer and two different Helium-Neon (HeNe) laser sources (632.8 nm and 3.39 μm). The spectrometer has the advantage of providing broad spectral transmittance measurements, but lacks the accuracy of some more direct measurements. Laser measurements, on the other hand, provide excellent accuracy at one frequency, but lack the spectral information of broadband approaches. Therefore, the combination of these two is synergistic.

Broadband transmittance measurements were performed from 500 nm to 7 μm using a Fourier Transform Spectrometer (BOMEM DA3.02) configured with a quartz-halogen lamp, quartz beamsplitter, and a silicon (Si) detector for the visible spectrum (500 to 850

nm). An MCT detector with a KBr beamsplitter and globar source were used for the mid-IR measurements (2 to 7 μm). The beam size at the sample location within the spectrometer was set to 3.5 mm, hence each measurement is representative of a spatial average of this size over the sample. The entire optical path of the spectrometer could be either evacuated or purged with nitrogen. Visible measurements were collected in the purge mode while the mid-IR measurements were conducted in evacuation mode to remove water absorption lines. Vacuum levels in the sample compartment between 0.08 and 0.5 Torr were typical.

The ultraviolet spectra between 180 nm and 500 nm were measured on a spectrometer (Cary 5G UV/VIS/NIR, VARIAN) set to scan from 185 nm to 400 nm at a rate of 500 nm/m. A holmium oxide reference filter was used to verify the spectrometer's performance. Before each sample analysis a background spectrum was collected as part of the instrument's baseline correction routine.

Laser measurements of transmittance were made at two HeNe laser wavelengths with a chopped beam. Measurements at 632.8 nm used a Si detector while measurements at 3.39 um used an InSb detector. In each case, the detectors subtended an acceptance angle of 0.7°. The transmittance was determined by taking the ratio of the transmitted power through a sample with the incident laser power without a sample. For each sample, ten laser transmittance measurements were taken at different locations and averaged to remove any local scattering effects. The standard deviation amongst the measurements on a single sample was typically 0.1%.

Optical phase functions representing the angular distribution of the scatter were performed to determine the bi-directional scatter distribution functions (BSDF). These measurements were performed with the visible HeNe laser. For the BSDF measurements, the source laser beam was chopped, expanded, and focused onto a detector mounted on a rail, which was in turn mounted on a rotational stage. The detector was rotated around the sample and the detector output recorded by a lock-in amplifier whose reference signal was derived from the chopper. The sample was mounted at the center of rotation of the detector-rail system and at a near-normal angle of incidence with respect to the incident beam. This provides complete characterization of the scatter intensity profile for each of the samples. For these measurements, polarization was ignored and we assumed that the scattered light is independent of sample rotation about the sample normal.

Samples for ballistic testing were hot pressed by TA&T. The 11" x 14" were hot-pressed in a 250 ton vacuum hot-press and then HIPed . The 5" diameter samples were hot-pressed in a 30 ton induction hot-pres and then HIPed . The spinel plates were ground and polished before laminating. Figure 3 shows some of the 11" x 14" spinel plates, after polishing, that were used in fabricating large test multi-hit test windows. The plates were laminated into transparent armor windows by ARL. V50 and multi-hit ballistic testing was conducted by ARL. A spinel based transparent armor window after multi-shot ballistic testing is shown alongside a front windshield mount for a HUMVE in Figure 4.

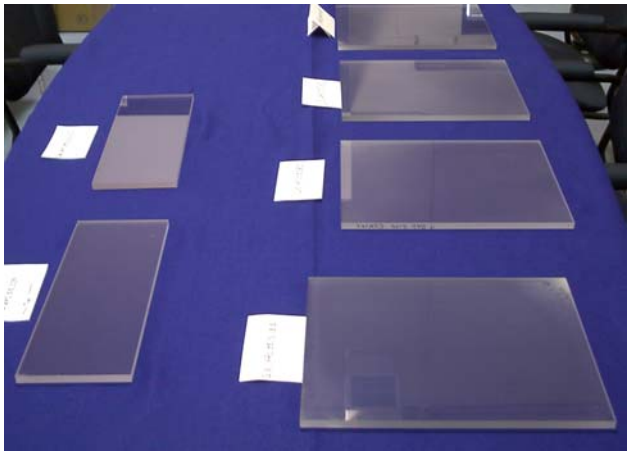

Figure 3 11" by 14" spinel plates used for ballistic testing

Figure 4. Multi-shot ballistic test sample shown with front windshield mount for HUMVE

III. Results and Discussion

The total transmittance through a material can be written as

$$T = \frac{(1-R)^2}{\left(1-R^2 e^{-2\beta_e L}\right)} e^{-\beta_e L}, \quad (1)$$

where $R = \left[(n-1)/(n+1)\right]^2$ is the single surface reflection coefficient, n is the index of refraction, L is

the material thickness, and β_e is the extinction coefficient. Solving for the extinction coefficient yields

$$\beta_e = \frac{1}{L}\times\ln\left(\frac{2R^2T}{\sqrt{(1-R)^4+4R^2T^2}-(1-R)^2}\right). \quad (2)$$

The refractive index is not expected to vary between the different spinel samples and can be written in terms of a Sellmeier model[1],

$$n = \sqrt{1+\frac{1.8938\lambda^2}{\lambda^2-0.09942^2}+\frac{3.0755\lambda^2}{\lambda^2-15.826^2}}\,. \quad (3)$$

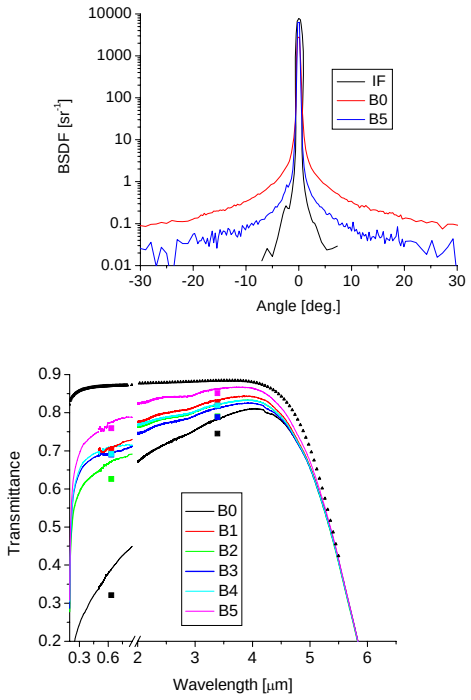

Fig. 5. Comparison of BSDF measurements for samples B0, B5, and the instrument function at 632.8 nm (left); and comparison of spectrometer and laser transmittance measurements of the B samples along with the ideal transmittance (triangles) derived from the Sellmeier model (above)

Note that the range of validity of this particular Sellmeier model is given as 0.35 to 5.5 μm. Temporarily limiting our analysis to the region where no intrinsic absorption occurs (from 0.35 to approximately 4 μm), the extinction is completely attributed to scatter. Because of this, there is an apparent mismatch between the laser and spectrometer measured transmittances. As was previously stated, the laser transmittance measurements subtended a half-angle of 0.7º. The spectrometer, on the other hand, is an f/4 system whose detectors subtend a 7.125º half-angle. This results in the spectrometer collecting a significant portion of scattered light and recording a higher transmittance. Evidence of this effect can be found in Fig. 5, which shows the measured transmittances of the B samples alongside the forward-scatter half of the BSDF of two of the samples (B0 and B5) measured at 632.8 nm. Also shown on the scatter plot is the instrument function (IF) of the BSDF system, which represents what an ideal sample with no scatter would look like. Of the samples, B5 has the narrowest scatter profile, although it is noticeably wider than the instrument function.

The most accurate assessment of the extinction coefficient comes from the laser transmittance measurements as these measurements incorporate the least amount of scattered light. The measured laser transmittances and corresponding extinction coefficients are listed in Table III and plotted in Fig. 6 as functions of the various HIP conditions for the three different hot-pressed billets. The uncertainty in these measurements is about 0.001 for the transmittance and 0.02 cm^{-1} for the extinction coefficient. Estimates of the broadband extinction coefficients of the samples (shown in Fig. 3) can be determined by applying a multiplicative scaling factor to the spectrometer transmittances, thereby matching them to the laser values at the appropriate wavelengths. As a check on the validity of this approach, we integrate the laser-measured BSDF plots over the field of view of the spectrometer (half-angle = 7.125º) as follows

$$T = \int_0^{2\pi} d\phi \int_{-\theta_{FOV}/2}^{\theta_{FOV}/2} BSDF(\theta)\sin(\theta)\,d\theta\,. \quad (4)$$

Table III. Comparison of Measured Transmittance and Extinction Coefficients

Sample	Length [cm]	Visible (632.8 nm)		Infrared (3.39 μm)	
		T ±0.001	β_e [cm^{-1}] ±0.02	T ±0.001	β_e [cm^{-1}] ±0.02
A0	0.607	0.329	1.59	0.755	0.26
A1	0.517	0.662	0.52	0.853	0.07
A2	0.521	0.711	0.39	0.833	0.11
A3	0.522	0.767	0.24	0.831	0.12
A5	0.521	0.824	0.10	0.866	0.04
B0	0.608	0.321	1.63	0.745	0.28
B1	0.519	0.702	0.41	0.827	0.13
B2	0.523	0.626	0.63	0.790	0.21
B3	0.517	0.690	0.45	0.788	0.22
B4	0.520	0.692	0.44	0.819	0.15
B5	0.520	0.759	0.26	0.851	0.07
C0	0.613	0.477	0.98	0.795	0.17
C1	0.520	0.690	0.44	0.827	0.13
C2	0.522	0.666	0.50	0.798	0.20
C3	0.524	0.767	0.24	0.813	0.16
C4	0.516	0.788	0.19	0.838	0.10
C5	0.524	0.826	0.10	0.845	0.09

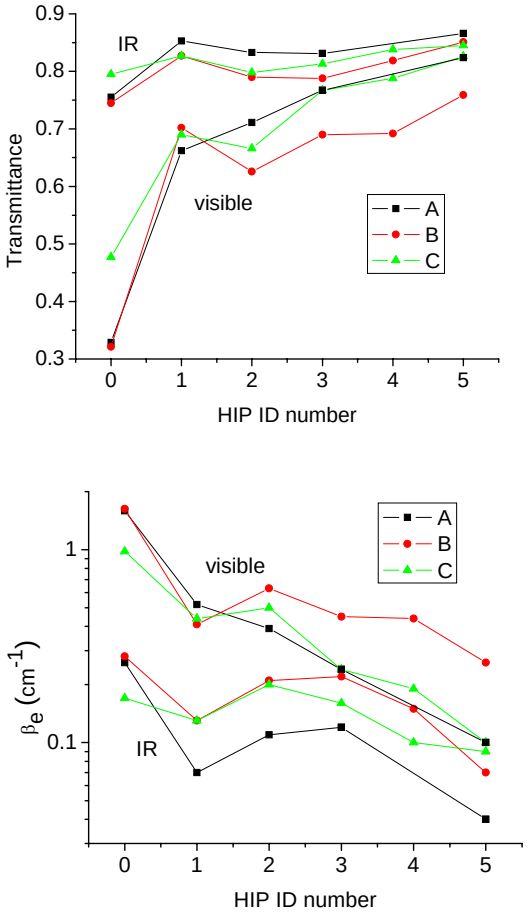

Fig. 6. Dependence of laser measured transmittance (left) and extinction coefficient (right) of three different billets (A, B, C) HIPed at various conditions (1-5). HIP ID 0 is a control and is only hot-pressed.

This check will be most accurate for the more highly scattering samples. For the B0 and C0 samples, the integrated transmittance over the spectrometer's field of view are 0.37 and 0.52, compared to direct spectrometer measurements of 0.36 and 0.51, respectively.

Upon examination of the data in Fig. 3, it is obvious that there are two main processes contributing to the extinction in these spinel samples. Our analysis focuses on the first region ($\lambda \leq 4\ \mu$m) where we attribute all extinction to scatter. As we progress further into the infrared, however, the effects of scatter become less apparent and intrinsic absorption takes over as the dominant extinction process. This absorption is characterized by both the complex index of refraction and multiphonon processes[6]. It will not be discussed further as the purpose of this paper is to compare various processing techniques and their effect on the extrinsic properties of spinel.

In order to more fully characterize the scatter coefficient of the spinel samples as a function of wavelength, we fit the extinction coefficient data in the IR (up to 4μm) to the power law relationship

$$\beta_e \approx \beta_s \propto \lambda^{-\nu}, \qquad (5)$$

where β_s is the scatter coefficient and ν is an empirical parameter. One such fit for each sample lot (A5, B5, and C5) is shown in Fig. 7. Inspection of the resulting exponent reveals information about the size, relative to the wavelength, of the structures responsible for scatter. In particular, if the wavelength is large with respect to the scatterers, one observes an exponent of four. This is referred to as the Rayleigh regime[7]. On the other hand, when the scatterers are large in comparison to the wavelength, the exponent approaches zero. This is known as the geometrical optics regime[7]. Shown in Fig. 8 are the results of this analysis performed on the samples. Here we see that the exponents are on the order of unity, which is consistent with a transition between the Rayleigh and geometrical optics regimes. This suggests that the structures responsible for scatter are much larger than the wavelengths of light. In addition, there is a general trend for the exponents to decrease from the as hot-pressed samples to those HIPed at 1900°C, suggesting that the size of the scattering sites is slightly increasing with increasing HIP temperatures.

The results of examination of the spinel using an optical microscope with transmitted light support these claims. Optical micrographs from the as hot-pressed sample as well as samples HIPed at 1500°C, 1700°C and 1900°C are shown in Fig. 9. As can be seen in the photographs, the decorated grain boundaries are on the order or 100 μm in the as hot-pressed spinel and increase in size with increasing HIP temperature. Additionally, there are many triple points and pore clusters in the as hot-pressed sample. As the HIP temperature was increased the frequency of decorated grain boundaries and triple points decreased. Pores, however, remained visible even at the hottest HIP temperature. This indicates that the dominant sources of scatter within the spinel are the decorated grain boundaries and triple points. As the HIP temperature is increased, the number of scattering sites decreases; those that remain increase in size. For specimens HIPed at 1500ºC there was no grain growth from the as hot-pressed condition. Those HIPed at 1700ºC showed moderate grain growth. The specimens HIPed at 1900ºC displayed massive grain growth. Making exact measurements of grain size was beyond the scope of this work.

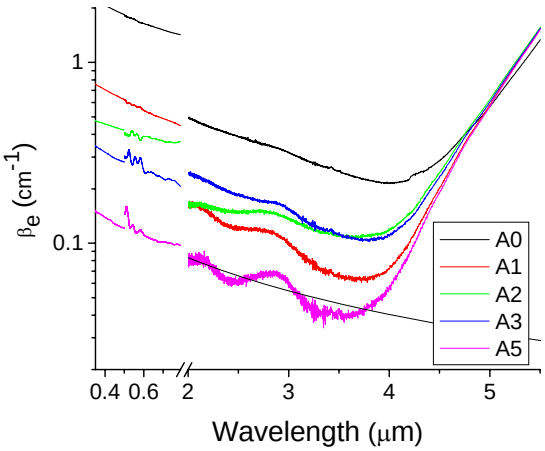

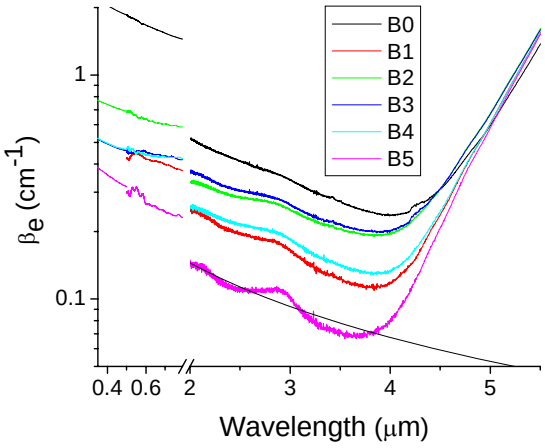

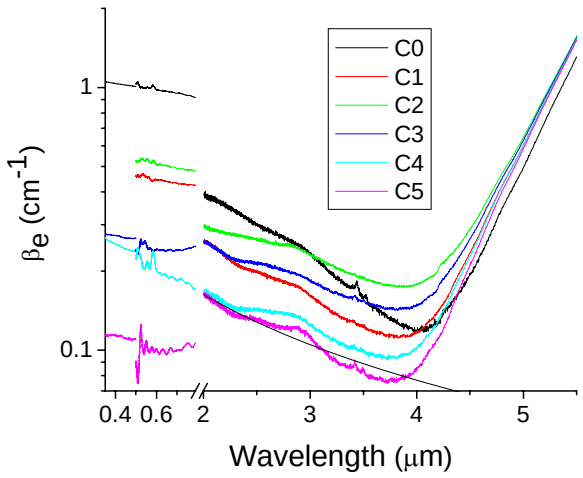

Fig. 7. Estimated broadband extinction coefficients vs. wavelengths

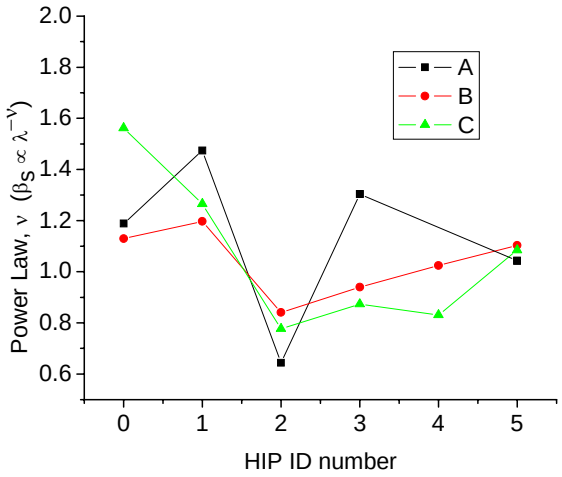

Fig. 8. Power law wavelength dependence of scatter cross-section for the samples.

The specifics of the ballistic testing are classified secret but general trends can be reported here.[8910] Single shot ballistic testing showed that spinel is 50% lighter than a traditional glass/plastic system. It ballistic performance is the same as ALON based systems. Both ALON and spinel which are polycrystalline ceramics are 10% better than sapphire based systems based on the single shot ballistic testing. Multi-hit ballistic testing has shown that sapphire is as good as spinel. This result was surprising because all the single shot testing clearly showed that sapphire was inferior to both spinel and ALON. The multi-hit performance of the sapphire and spinel based systems were only 33% better than traditional glass/plastic based systems. Spinel for ballistic testing was HIped at 1900°C. The microstructure of the spinel HIPed at this temperature is extremely coarse. This course microstructure gives the best optical transmission and did not have a deleterious effect on the single shot ballistic performance of spinel.

IV. CONCLUSIONS

In this study, the optical properties of spinel were compared for varying hot-pressing and HIP conditions. Specifically, the optical transmittance was measured and the extrinsic scatter coefficient calculated, which dominates the extinction from the UV to about 4 μm. Samples were initially hot pressed at either 1620°C (A) or 1650°C (B) with an additional set of sample B pieces receiving a 1550°C, 12 hour anneal (C). Samples

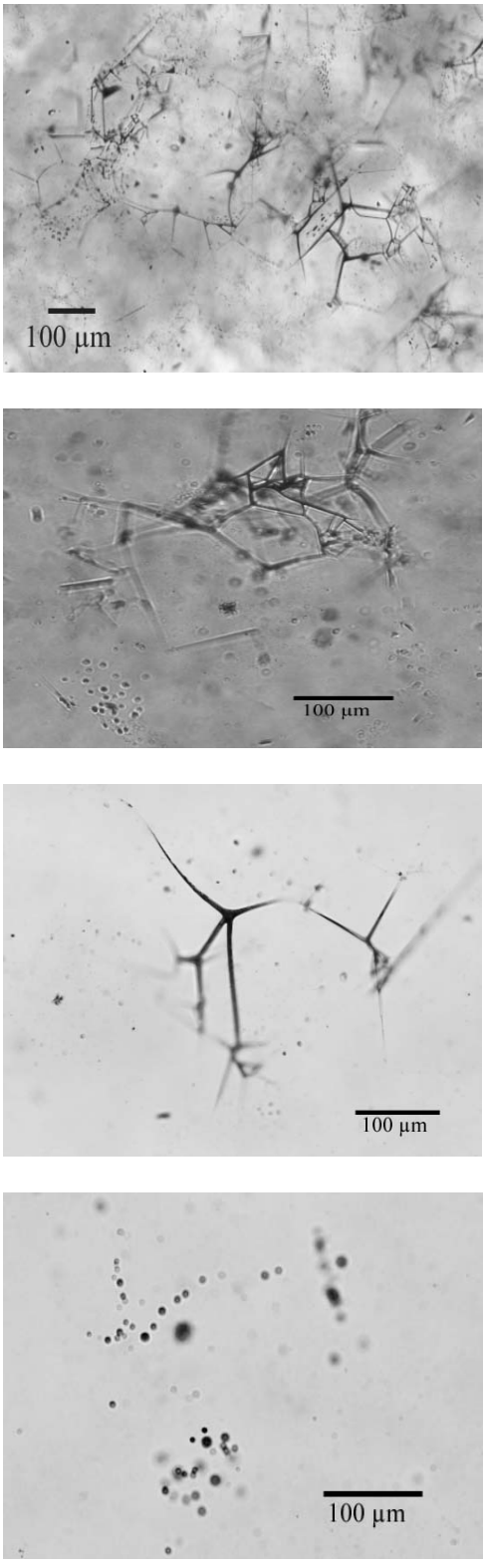

.**Fig. 9.** Optical Micrographs showing defects such as pore clusters, decorated grain boundaries and tripplepoints in spinel using transmitted light. Top as hot-pressed, 2nd HIPed 1500°C, 3rd HIPed 1700°C, and bottom HIPed 1900°C.

from these three lots were then subjected to five different HIP processing conditions with pressures of either 100 or 200 MPa and temperatures ranging from 1500°C to 1900°C. Results indicated slight increases in scatterer size with increasing HIP temperatures and pressures.

It was concluded that the lower hot-pressing temperature (A) provided the best optical properties for all five of the varying HIP conditions. It was also shown that the 1650°C as hot-pressed samples subjected to the anneal (C) had noticeably lower scatter than the unannealed samples (B). Results from the various HIP conditions indicate that there is some benefit to increasing the HIP temperature and pressure for reducing the extinction coefficient in the visible. In the IR, this benefit was less noticeable; HIP temperatures of 1900°C produced only slightly better optical properties than those of 1500°C. In both the visible and IR, the lowest extinction coefficients were found at the highest HIP temperature (1900°C).

To better understand these results, broadband power law fitting was applied to the scatter coefficients and optical micrographs of the samples were taken. Results from the power law fitting indicate slight increases in scatterer size with increasing HIP temperatures and pressures. The fit exponent of about one is representative of the mean scatterer size being much larger than the optical wavelength, in this case 4 μm. Optical microscopy revealed the presence of decorated grain boundaries, decorated triple points, and pore clusters. The grain boundaries and triple points are decorated with LiF that was not removed during the hot-pressing cycle. Pores were generally found in clusters indicating that they are result of agglomerates in the starting powder. The micrographs show grain sizes of about 100 μm for the hot-pressed samples that grow to 200-300 μm at the greatest HIP pressures and temperatures. In contrast, the pore sizes remained relatively constant for all processing conditions at less than about 10 μm. For this reason, we attribute the major cause of optical scatter to the presence of LiF at the grain boundaries. The primary goal of this research was to determine whether HIPing at low temperature could produce a good optically transparent spinel. The results show that HIPing at 1500ºC can produce a good optically transparent spinel for use in the mid-IR. For use in the visible wavelengths spinel requires HIPing at higher temperatures. Future work will concentrate on reducing the concentration of LiF and varying grain size to further reduce extrinsic scattering in spinel.

Ballistic testing is underway to determine if the multi-hit ballistic performance of ALON is the same as sapphire and spinel. Spinel plates 11” x 14” have been hot-pressed and HIPed at 1700°C to determine the effect of a finer microstructure on the multi-hit ballistic

performance. Figure 10 shows how the microstructure can be refined by using a lower HIP temperature.

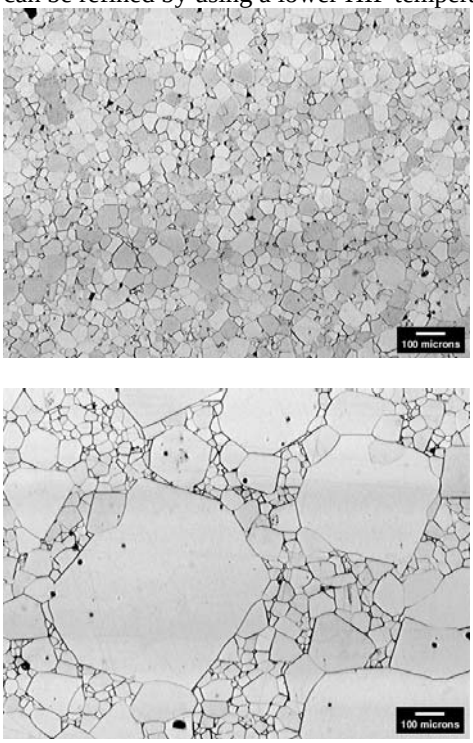

Figure 10. Top micrograph shows finer grained spinel HIPed at 1700C bottom micrograph shows spinel HIPed at 1900C.

Increasing the size and reducing the cost of ceramics for transparent armor will allow us to provide greater protection at reduced weights to the warfighter. Transparent armor is a critical technology in protecting the soldier. As seen in Figure 11.

Figure 11. Transparent armor in use in Iraq.

REFERENCES

[1] Harris, D. C., Materials for Infrared Windows and Domes, Properties and Performance, SPIE Press, Bellingham, Washington, 1999.

[2] M.E. Thomas, R.L. Joseph and W.J. Tropf, "Infrared Properties of Sapphire, Spinel and Yttria as a Function of Temperature", SPIE vol. 683, 1986.

[3] J.A. Cox, D. Greenlaw, G. Terry, K. McHenry and L. Fielder, "Infrared and Optical Transmitting Materials", SPIE vol. 683, 1986

[4] G. Gilde, P. Patel, M. Patterson, "A comparison of Hot-Pressing, Rate controlled Sintering and Microwave Sintering of Magnesium Aluminate Spinel for Optical Applications", Window and Dome Technologies and Materials VI, R.W. Tustison, Volume 3705, 1999 Proceedings of SPIE, Washington, USA

[5] D.W. Roy, M. C.L. Patterson, J. E. Caiazza, G. Gilde, "Progress In Development Of Large Transparent Spinel Plates", Proceedings 8th DoD Electromagnetic Windows Symposium, April 2000

[6] M. E. Thomas, R. I. Joseph, and W. J. Tropf, "Infrared transmission properties of sapphire, spinel, yttria, and ALON as a function of temperature and frequency," *Applied Optics*, Vol. 27, No. 2, p. 239-245, 1988.

[7] M. E. Thomas and D. D. Duncan, Chapter 1 in *The Infrared & Electro-Optical Systems Handbook, Volume 2, Atmospheric Propagation of Radiation*, (F. G. Smith ed.), SPIE Optical Engineering Press, Ann Arbor, MI, p. 97-99, 1993

[8] Parimal J. Patel, Gary Gilde "Development of a Lightweight Transparent Armor System, Part II," P. J. Patel, G.Gilde, ARL-TR-3821 , 06/01/2006

[9] Parimal J. Patel, Gary Gilde "Comparison of AlON, Spinel and Sapphire for Transparent Armor Applications," P. J. Patel, G. Gilde, ARL TR-xxxx, est. 09/2006

[10] Parimal J. Patel, Gary Gilde "Development of a Lightweight Transparent Armor System, Part I," P J. Patel, G. Gilde, ARL TR 3466, April 2005.